Adaptive Robust Control for Maximum Power Point Tracking in Photovoltaic Systems based on Sliding Mode and Fuzzy Control

Case Study

Minh Van Pham
Faculty of Electricity and Automation, University of Economics-Technology for Industries
Minh Khai Street, Ha Noi City, Vietnam
pvminh@uneti.edu.vn
*Corresponding author

Abstract *– Photovoltaic (PV) systems play a crucial role in renewable energy generation, but their efficiency heavily depends on accurate Maximum Power Point (MPP) tracking under varying environmental conditions. This paper applies an adaptive robust controller (ARC) to improve MPP tracking performance in PV systems, with a particular focus on enhancing robustness and reducing chattering. First, a sliding surface is defined based on the maximum power point. Then, a sliding mode controller is designed to ensure robustness against system uncertainties and external disturbances. To mitigate the chattering effect, a fuzzy logic-based controller is integrated into the ARC framework. The proposed controller is proven to be stable according to the Lyapunov criterion, providing robustness to uncertain parameters and external disturbances and reducing chattering. The proposed controller is validated through comparative simulations, demonstrating its superior performance over conventional methods. The results demonstrate that the proposed ARC achieves faster convergence, higher tracking accuracy, and improved robustness compared to conventional methods. Moreover, the integration of fuzzy logic significantly mitigates chattering, enhancing system efficiency and reliability. Given these advantages, the proposed controller is well-suited for real-world PV energy conversion systems, particularly in environments with rapidly changing irradiance and temperature conditions.*

Keywords*: adaptive, robust, maximum power point tracking (MMPT), fuzzy controller, sliding mode control, photovoltaic systems*

Received: February 27, 2025; Received in revised form: June 4, 2025; Accepted: June 5, 2025

1. INTRODUCTION

Renewable energy has become a crucial component in electricity generation, with photovoltaic (PV) and wind energy being widely utilized for power production. Among these, PV systems stand out due to their availability and environmental benefits, making them a viable clean energy source [1]. PV technology has been extensively adopted across various fields, including agriculture, industry, and services [1-3].

PV systems exhibit a maximum power point (MPP) that varies with environmental conditions such as temperature and solar irradiance. The primary function of the controller is to ensure that the PV system continuously operates at the MPP. An effective controller must not only accurately track the MPP but also maintain adaptability and robustness under different operating conditions. Maximum power point tracking (MPPT) techniques can be broadly categorized into indirect and direct methods. Indirect MPPT algorithms rely on pre-established PV characteristics or mathematical relationships with environmental parameters. Consequently, their tracking accuracy is limited across varying temperature and irradiance levels [3]. Additionally, utilizing temperature and irradiance parameters as control inputs introduces several constraints [4]. In contrast, direct MPPT methods can adapt to all weather conditions, making them the preferred approach. The perturbation and observation (P&O) and incremental conductance (INC) algorithms are the most widely used direct MPPT techniques due to their simplicity and ease of implementation. However, these methods struggle with rapid irradiance fluctuations and often result in power oscillations around the MPP when irradiance is stable [2, 5, 6]. Advanced MPPT strategies based on fuzzy logic (FL) or artificial neural networks (ANN) have also been investigated, but their complexity is higher compared to conventional MPPT algorithms, which are typically simple and cost-effective [7, 8].

MPPT strategies are primarily implemented using a two-loop control scheme, where the first loop determines the reference voltage, and the second loop ensures that the PV system follows this reference voltage. The tracking performance is heavily dependent on the controller in the second loop, which must effectively handle system nonlinearities, uncertainties, and external disturbances. A common drawback of most MPPT methods is the occurrence of power chattering around the MPP. An ideal MPPT controller should not only accurately track the MPP under all conditions but also mitigate nonlinearities and uncertainties. Sliding mode control (SMC) is a nonlinear control technique well-known for its robustness against system uncertainties and external disturbances. It offers a high degree of flexibility in control design, making it a strong candidate for MPPT applications. In [9], an SMC-based MPPT scheme is proposed where the reference voltage is obtained using the P&O algorithm, and a sliding mode controller is employed to track this voltage. Similarly, an end-to-end SMC approach was introduced in [10], where the INC algorithm determines the MPP, and an SMC is used for tracking. However, both methods fail to eliminate chattering. To address this, an adaptive sliding controller with an automatically adjusted switching factor was proposed in [11], effectively reducing chattering. Unfortunately, this approach does not account for external disturbances and parameter uncertainties.

An alternative approach is the use of a single-loop SMC for MPPT, where the sliding surface is directly defined based on the MPP, simplifying the control structure and improving efficiency compared to two-loop methods [12]. In [13], a sliding mode-based MPPT controller was developed, however, it did not fully eliminate chattering. More advanced solutions have explored the integration of sliding mode control with fuzzy logic techniques to mitigate chattering; however, these approaches often neglect the effects of system uncertainties and external disturbances.

Recently, several enhanced MPPT techniques have been proposed to improve tracking performance under challenging environmental conditions. In [14], Jately et al. conducted an experimental analysis of hill-climbing MPPT algorithms under low irradiance levels, highlighting the limitations of conventional methods in maintaining efficiency during partial shading or reduced sunlight. Meanwhile, Jately and Arora [15] investigated the performance of various hill-climbing techniques under rapidly changing environmental conditions, showing that while these methods offer fast response, they may suffer from oscillations around the MPP. More recently, Jamshidi et al. [16] proposed an improved sliding mode controller that enhances MPPT accuracy in dynamic environments. Their method demonstrates strong robustness and tracking precision; however, it still faces challenges related to chattering suppression and implementation complexity in real-world systems.

These recent developments indicate that while progress has been made in enhancing tracking performance and robustness, a clear research gap still exists: there is a lack of MPPT control strategies that simultaneously ensure (i) high robustness against uncertainties, (ii) effective chattering suppression, and (iii) structural simplicity via a single-loop implementation. To address this, this paper proposes an adaptive robust controller (ARC) for MPP tracking, integrating sliding mode control and fuzzy logic in a single-loop structure. The SMC component ensures system stability and robustness against parameter variations and external disturbances, while the fuzzy controller effectively eliminates chattering. This approach is expected to enhance MPPT performance, offering a potentially more reliable and efficient solution for PV energy conversion systems.

2. MATHEMATICAL MODEL OF THE SYSTEM AND PROBLEM FORMULATION

2.1. MODELING OF PV SYSTEM

The PV system can be represented based on a PV equivalent circuit. Commonly used equivalent circuits are single-diode models [17, 18] or double-diode models [19, 20]. Consider the single diode model shown in Fig. 1, where I_{ph} is a current source, I_d is a diode representing the polarization phenomenon, R_s is a resistor representing the various contact and connection resistances, and R_p is a resistor representing the various leakage currents.

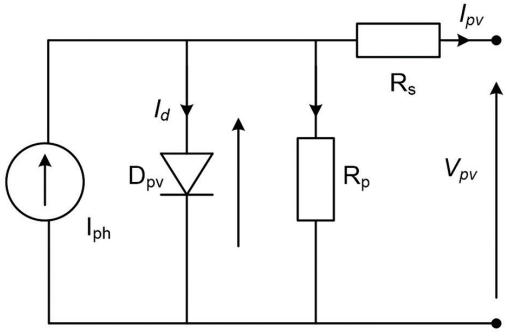

The mathematical model of PV array is given as follows [21, 22]:

$$I_{pv} = N_P I_{ph} - N_P I_s \exp\left(\frac{V_{pv} + \beta R_s I_{pv}}{N_s \delta V_T} - 1\right) - \frac{V_{pv} + \beta R_s I_{pv}}{\beta R_p} \quad (1)$$

where N_s is the number of solar panels connected in series, N_p is the number of solar panels connected in parallel, I_s is the reverse saturation current, and I_{ph} is the photo-current, $\beta = N_s/N_p$, I_{pv} is the output current of the PV array, V_{pv} is the output voltage of the PV array, and δ is the ideality factor. In practice, R_s often has a minimal value, and R_p has a very large value. Therefore, equation (1) is rewritten as follows:

$$I_{pv} = N_P I_{ph} - N_P I_s \exp\left(\frac{V_{pv}}{N_s \delta V_T} - 1\right) \quad (2)$$

The PV model used in this paper is based on a single-diode equivalent circuit, and the following assumptions are considered to simplify the mathematical representation [21, 22]:

1. The shunt resistance R_p is assumed to be very large and thus its effect is neglected.

2. The series resistance R_s is retained but considered constant and temperature-independent.

3. The effect of changes in temperature and irradiance is reflected through I_{ph}, I_s, and V_{pv}, which are calculated at standard test conditions (STC).

4. The diode ideality factor δ, thermal voltage, and saturation current I_s are assumed constant for a given condition.

5. The influence of partial shading and aging of solar panels is neglected.

Consider a specific PV system consisting of 5 Sun Power SPR-305E-WHT-D panels connected in series per string and 66 parallel strings used [11]. The specifications of the Sun Power SPR-305E-WHT-D PV panels are as follows: maximum power is 305.226W, open circuit voltage V_{oc}=64.2V, short-circuit current I_{sc}=5.96A, voltage at maximum power point V_{mp}=54.7V, current at maximum power point I_{mp}=5.58A. This PV system delivers a maximum power of 100 kW under irradiance and temperature conditions. The I-V and P-V characteristics of the PV system under different irradiance conditions are shown in Fig. 2.

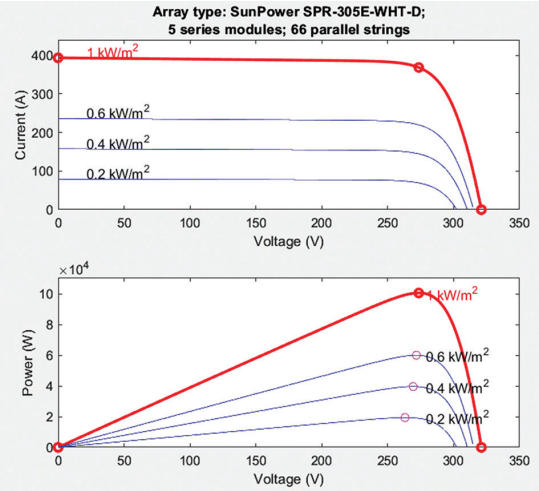

Fig. 2. I-V and P-V characteristics of PV system

2.2. DC/DC BOOST CONVERTER

DC/DC converter is an indispensable part of the PV system, and it is connected to adjust the output voltage of the PV system. Commonly used DC/DC converters are buck converter, boost converter, and buck-boost converter. In this paper, a boost converter is used. The schematic diagram of the boost converter circuit is shown in Fig. 3, in which V_{pv} is the input voltage, V_o is the output voltage, I_L is the induced current, R is the circuit load, u has a value in the range [0,1] is the pulse width of PWM (Pulse Width Modulation) stage. The values of inductor components L, input capacitor C_v, and output capacitor C_o are selected as follows [11]: L=0.005H, C_v=5.10^{-3} F, C_o=5.10^{-3} F, R=4.9 Ω, PWM switching frequency is chosen as 5000Hz.

The circuit operates in two cases: when K is conducting and when K is in the off state. The state equations of I_L and V_o are as follows [9, 19]:

$$\dot{I}_L = \frac{V_{pv} - V_o}{L} + \frac{V_o}{L}u + \zeta \tag{3}$$

$$\dot{V}_o = \left(\frac{-V_o}{RC_o} + \frac{I_L}{C_o}\right) - \frac{I_L}{C_o}u \tag{4}$$

where ζ represents the uncertain parts of the system arising from measurement errors, values of passive components, and loads. ζ satisfies the following conditions [9]:

$$|\zeta| \le b_\zeta \tag{5}$$

where b_d is a positive constant. Defining φ=[I_L, V_0]^T, we get the following dynamic equation:

$$\dot{\varphi} = f(\varphi) + g(\varphi)u + k(\varphi)\zeta \tag{6}$$

where $f(\varphi) = \left[\frac{V_{pv} - V_o}{L}, \frac{-V_o}{RC_o} + \frac{I_L}{C_o}\right]^T$, $g(\varphi) = \left[\frac{V_o}{L}, -\frac{I_L}{C_o}\right]^T$, $k(\varphi) = [1,0]^T$, $u \in [0,1]$.

The mathematical model of the boost converter is developed under the following assumptions [21, 22]:

1. All circuit components (inductor L, capacitor C, switch, diode) are ideal and lossless.
2. The converter operates in continuous conduction mode (CCM).
3. The switching is instantaneous and perfectly synchronized with the PWM signal.
4. Parasitic elements and switching losses are ignored.
5. The output load is resistive and constant during operation.

2.3. PROBLEM FORMULATION

The objective of the problem is to design ARC for system (8) with the impact of ζ, ensuring that the system always operates at the MPP. The control system structure diagram is shown in Fig. 4.

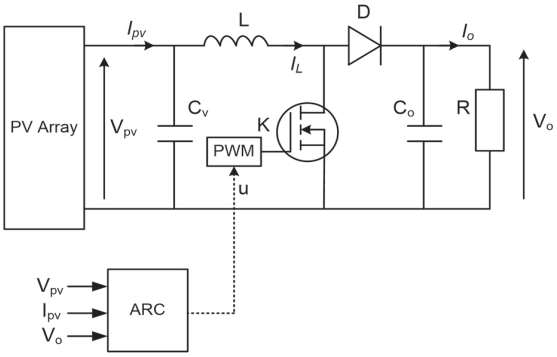

Fig. 4. Control system structure diagram

3. ADAPTIVE ROBUST CONTROLLER DESIGN

This section designs the ARC controller, which includes a sliding mode controller and a fuzzy controller, where the fuzzy controller is used to select the switching coefficient to reduce the chattering phenomenon.

3.1. SLIDING MODE CONTROLLER

As observed in Fig. 2, when the system operates at its MPP, the slope of the P-V characteristic is zero. Therefore, we have

$$\frac{\partial P_{pv}}{\partial V_{pv}} = I_{pv} + V_{pv}\frac{\partial I_{pv}}{\partial V_{pv}} = 0 \tag{7}$$

The definition of sliding surface is as follows [12, 23]:

$$\overline{s} = \frac{\partial P_{pv}}{\partial V_{pv}} \tag{8}$$

The sliding mode controller is designed as equation (9), consisting of 2 components, u_{SMC} to pull the system state to the sliding surface, u_{td} to ensure the state remains on the sliding surface and moves towards the origin.

$$u = u_{SMC} + u_{td} \tag{9}$$

The control law is designed as follows:

$$u = \left(1 - \frac{V_{pv}}{V_o}\right)\left(-\frac{L}{V_o}\kappa\,\mathrm{sgn}(S)\right) \tag{10}$$

where $u_{SMC} = \left(1 - \frac{V_{pv}}{V_o}\right)$, $u_{td} = -\frac{L}{V_o}\kappa\,\mathrm{sgn}(S)$, $|\kappa| \geq b_\zeta$.

Choose a Lyapunov function as follows:

$$L = \frac{1}{2}\overline{s}^2, \tag{11}$$

Taking the derivative (11), we get

$$\dot{L} = \overline{s}\,\dot{\overline{s}}, \tag{12}$$

We have

$$\dot{\overline{s}} = \left(\frac{\partial \overline{s}}{\partial \varphi}\right)^T \dot{\varphi} = \left(\frac{\partial \overline{s}}{\partial I_{pv}}\right)^T \left(-\frac{V_o}{L}(1-u) + \frac{V_{pv}}{L} + \zeta\right), \tag{13}$$

The first component of equation (13) satisfies [13, 23]

$$\frac{\partial \overline{s}}{\partial I_{pv}} > 0. \tag{14}$$

Substituting expression (10) into equation (13), the second component of equation (13) becomes

$$-\frac{V_o}{L}(1 - u_{SMC} - u_{td}) + \frac{V_{pv}}{L} + \zeta = -\frac{L}{V_o}\kappa\,\mathrm{sgn}(\overline{s})) + \zeta \tag{15}$$

From equations (13) and (15), note (14) and $|\kappa| \geq b_\zeta$ we have

$$\dot{L} = \overline{s}\,\dot{\overline{s}} = \overline{s}\left(\frac{\partial \overline{s}}{\partial I_{pv}}\right)^T \left(-\frac{L}{V_o}\kappa\,\mathrm{sgn}(\overline{s})) + \zeta\right) < 0 \tag{16}$$

Thus, according to the Lyapunov stability criterion, we can conclude that the system is stable.

3.2. FUZZY CONTROLLER

The control law (10) shows that the larger the κ coefficient, the faster the states will approach the sliding surface and the higher the stability. However, the larger this coefficient is, the stronger the chattering phenomenon will be. The discontinuous switching nature of classical SMC often induces high-frequency oscillations (chattering), which can excite unmodeled dynamics and degrade system performance. While conventional chattering reduction methods exist, they frequently trade off robustness or increase control complexity. In contrast, fuzzy logic controllers generate smooth control signals through continuous membership functions and fuzzy inference mechanisms, thereby replacing the abrupt switching with gradual transitions. This smoothness significantly mitigates chattering without compromising the robustness and finite-time convergence properties guaranteed by SMC. Moreover, fuzzy logic's model-free and adaptive characteristics allow it to intelligently adjust the switching gain near the sliding surface, reducing excessive switching intensity that causes chattering while preserving the high-gain control action necessary when the system state is far from the sliding manifold. This adaptive tuning of the switching gain via fuzzy logic complements the inherent robustness of SMC against parameter variations and external disturbances. Therefore, integrating fuzzy logic with SMC in a single-loop ARC structure not only preserves system stability and robustness but also effectively mitigates chattering by adaptively modulating the switching gain. This leads to enhanced MPPT performance with reduced control complexity.

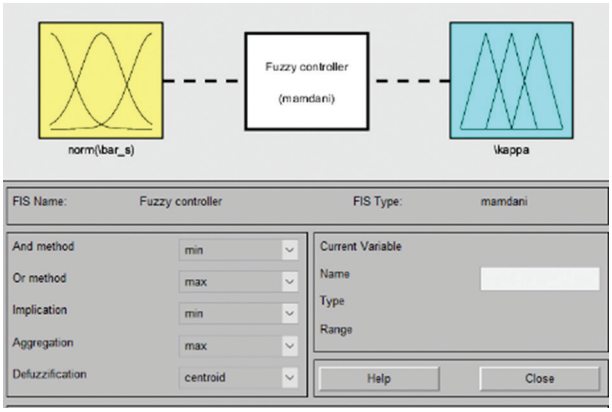

Fig. 5. Fuzzy controller structure: Number of inputs, outputs, composition rules, and defuzzification methods

The designed fuzzy controller includes a sliding surface input and an coefficient output. The structure of the fuzzy controller is illustrated in Fig. 5, The structure of the fuzzy controller is illustrated in Fig. 5, where the input and output membership functions are Gaussian-

shaped, as shown in Figs. 6 and 7, and the control rules are presented in Fig. 8.

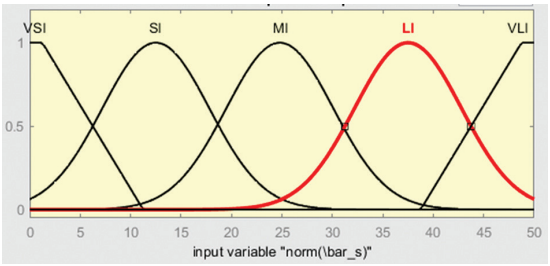

Fig. 6. Input membership function

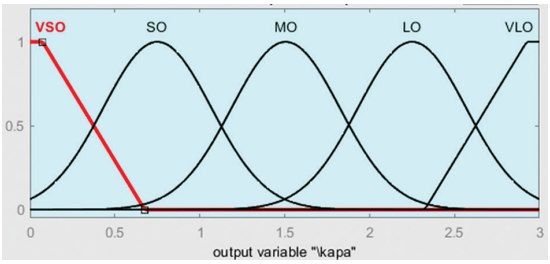

Fig. 7. Output membership function

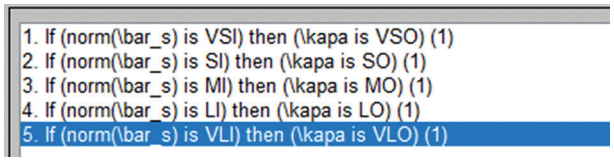

Fig. 8. Control rules

4. RESULTS

This section presents simulation results on Matlab software. The system operates under irradiance conditions varying in the range of [1000,200,600] W/m^2, temperature at 25°C, and the system's uncertainties caused by measurement errors are random values within the range [0,5]. The PV power, PV voltage, and PV current of ARC are shown in Figs. 9, 10, and 11. The output power corresponding to the ARC is depicted in Fig. 12. Although the radiation changes rapidly, ARC still ensures the quality of control. The system works stably with a response time of about 0.02s. The simulation results show that ARC provides good control quality and ensures working at the maximum power point.

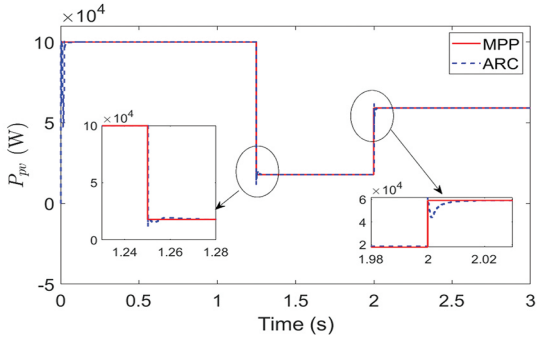

Fig. 9. Result of PV power

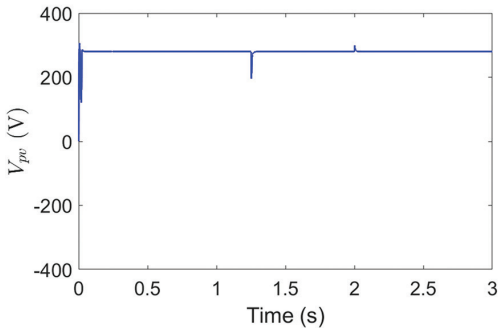

Fig. 10. Result of PV voltage

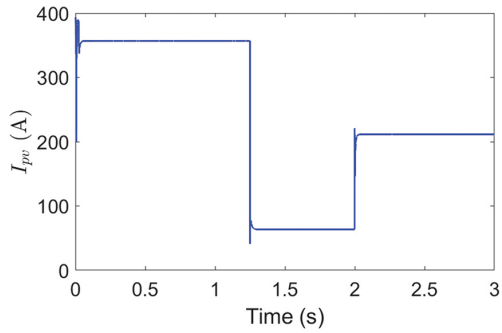

Fig. 11. Result of PV current

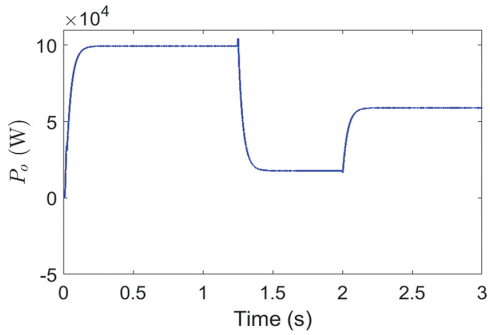

Fig. 12. Result of output power

To demonstrate the effectiveness of the RAC method, a comparison is conducted with the algorithms proposed in [24] and [25]. Fig. 13 illustrates the MPP tracking performance of the proposed ARC compared with Algorithm [24] and Algorithm [25].

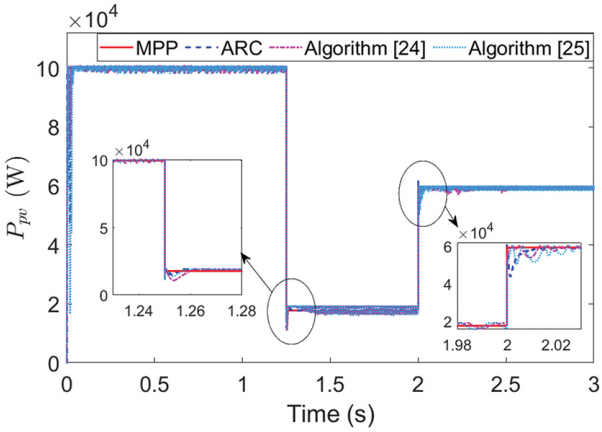

Fig. 13. PV power of the algorithms

At each irradiance transition point, the ARC closely follows the reference MPP curve with negligible deviation. In contrast, Algorithm [24] exhibits slight oscillations near the new MPP at $t = 1.25$ s, while Algorithm [25] shows more pronounced oscillations, especially at $t = 2$ s, where noticeable overshoot and undershoot occur. These observations confirm that ARC achieves tracking accuracy comparable to Algorithm [24], while significantly improving stability and reducing chattering compared to both Algorithms [24] and [25]. This improvement is attributed to the fuzzy-based adaptive gain adjustment, which minimizes unnecessary switching near the sliding surface.

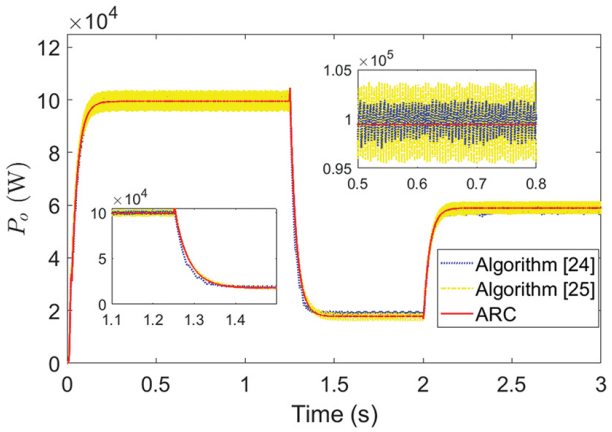

Fig. 14. Output power of the algorithms

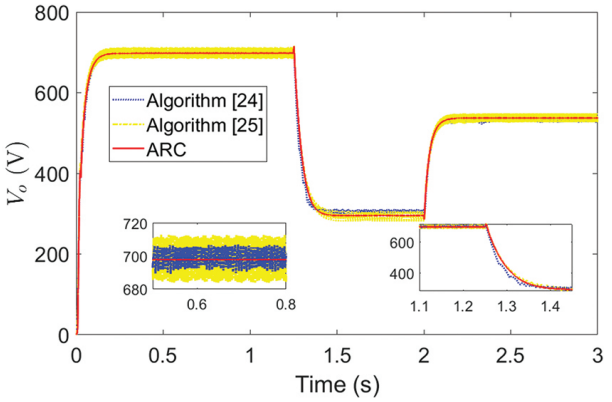

Fig. 15. Output voltage of the algorithms

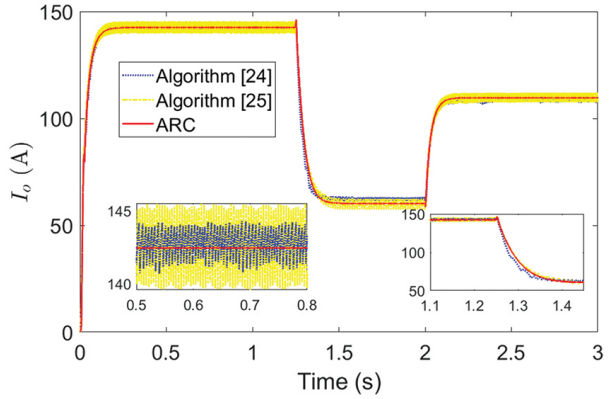

Fig. 16. Output current of the algorithms

Additionally, Figs. 14, 15, and 16 illustrate the output power, output voltage, and output current of the algorithms, respectively. These figures clearly demonstrate that the proposed ARC significantly reduces chattering compared to Algorithms [24] and [25], resulting in smoother and more stable system responses. Specifically, the output voltage of the ARC exhibits a peak-to-peak oscillation of only about 1 V, whereas Algorithm [24] reaches up to 16 V and Algorithm [25] up to 30 V. The peak-to-peak amplitude refers to the difference between the maximum and minimum values of the oscillating signal.

The dynamic efficiency of the simulated algorithms, computed using (17) in accordance with the method described in [20], is summarized in Table 1. The dynamic efficiency of the simulated algorithms, computed using (17) in accordance with the method described in [24], is summarized in Table 1. In addition, Table 1 also presents the response time and the output voltage chattering amplitude of the system.

$$Dynamic\ Efficiency = \frac{\int_0^T P_{PV}}{\int_0^T P_{MPP}}, \tag{17}$$

Table 1. Performance evaluation indices of the algorithms

Algorithm	Overall efficiency	Response time	Chattering amplitude
RAC	99.61%	10ms	1V
Algorithm [24]	98.59%	20ms	16V
Algorithm [25]	97.99%	15ms	30V

5. CONCLUSIONS

This paper has introduced an adaptive robust controller (ARC) for maximum power point tracking of photovoltaic systems. Comparative simulation results show that the proposed controller ensures robustness and good tracking quality. In addition, the controller has a simple structure because it only uses one loop. Therefore, one can easily deploy the algorithm on embedded devices. However, the current study presents some limitations. Firstly, the effectiveness of the controller has only been validated through simulation. Secondly, the proposed method assumes partial knowledge of system parameters and neglects component-level uncertainties in the boost converter and PV module. Future work will focus on extending the proposed ARC to systems with unknown or time-varying parameters. Additionally, experimental validation will be conducted to verify the feasibility and performance of the proposed method on a physical PV system prototype, thereby bridging the gap between simulation and practical implementation.

6. REFERENCES

[1] B. Parida, S. Iniyan, R. Goic, "A review of solar photovoltaic technologies", Renewable and Sustainable Energy Reviews, Vol. 15, 2011, pp. 1625-1636.

[2] T. Esram, P. L. Chapman, "Comparison of Photovoltaic Array Maximum Power Point Tracking Techniques", IEEE Transactions on Energy Conversion, Vol. 22, No. 2, 2007, pp. 439-449.

[3] V. Salas, E. Olías, A. Barrado, A. Lazaro, "Review of the maximum power point tracking algorithms for stand-alone photovoltaic systems", Solar Energy Materials and Solar Cells, Vol. 90, 2006, pp. 1555-1578.

[4] N. Femia, G. Petrone, G. Spagnuolo, M. Vitelli. "Power Electronics and Control Techniques for Maximum Energy Harvesting in Photovoltaic Systems", CRC press, 2012.

[5] D. Hohm, M. Ropp, "Comparative Study of Maximum Power Point Tracking Algorithms", Progress in photovoltaics: Research and Application, Vol. 11, 2003, pp. 47-62.

[6] D. Sera, L. Mathe, T. Kerekes, S. Spataru, R. Teodorescu, "On the Perturb-and-Observe and Incremental Conductance MPPT Methods for PV Systems", IEEE Journal of Photovoltaics, Vol. 3, 2013, pp. 1070-1078.

[7] B. Bendib, F. Krim, H. Belmili, A. Fayçal, B. Sabri, "An intelligent MPPT approach based on neural-network voltage estimator and fuzzy controller, applied to a stand-alone PV system", Proceedings of the IEEE International Symposium on Industrial Electronics, Istanbul, Turkey, 1-4 June 2014, pp. 404-409.

[8] J.-K. Shiau, Y.-C. Wei, B.-C. Chen, "A Study on the FuzzyLogic-Based Solar Power MPPT Algorithms Using Different Fuzzy Input Variables", Algorithms, Vol. 8, 2015, pp. 100-127.

[9] A. Hameed, H. S. Zad, A. Ulasyar, J. Hashim, "Robust Sliding Mode MPPT control of a Photovoltaic System", Proceedings of the 3rd International Conference on Computing, Mathematics and Engineering Technologies, Sukkur, Pakistan, 29-30 January 2020.

[10] C.-S. Chiu, Y.-L. Ouyang, C.-Y. Ku, "Terminal sliding mode control for maximum power point tracking of photovoltaic power generation systems", Solar Energy, Vol. 86, 2012 pp. 2986-2995.

[11] M. R. Mostafa, N. H. Saad, A. A. El-sattar, "Tracking the maximum power point of PV array by sliding mode control method", Ain Shams Engineering Journal, Vol. 11, 2020, pp. 119-131.

[12] A. Belkaid, J. P. Gaubert, A. Gherbi, "An Improved Sliding Mode Control for Maximum Power Point Tracking in Photovoltaic Systems", Journal of Control Engineering and Applied Informatics, Vol. 1, 2016, pp. 86-94.

[13] A. Kchaou, A. Naamane, Y. Koubaa, N. M'sirdi, "Second order sliding mode-based MPPT control for photovoltaic applications", Solar Energy, Vol. 155, 2017, pp. 758-769.

[14] V. Jately et al. "Experimental Analysis of hill-climbing MPPT algorithms under low irradiance levels", Renewable and Sustainable Energy Reviews, Vol. 150, 2021, pp. 111467.

[15] V. Jately, S. Arora, "Performance investigation of Hill-Climbing MPPT techniques for PV systems under rapidly changing environment", Intelligent Communication, Control and Devices: Proceedings of ICICCD 2017, Springer, 2018.

[16] F. Jamshidi et al. "An improved sliding mode controller for MPP tracking of photovoltaics", Energies, Vol.16, No. 5, 2023, p. 2473.

[17] M. Azzouzi, "Optimization of Photovoltaic Generator by Using P&O Algorithm under different weather conditions", Journal of Control Engineering and Applied Informatics, Vol.15, No.2, 2013, pp. 12-19.

[18] A. H. Besheer, A. M. Kassem, A. Y. Abdelaziz, "Single-diode model based Photovoltaic module: Analysis and comparison approach", Electric Power Components and Systems, Vol. 42, No. 12, 2014, pp. 1289-1300.

[19] F. Petcuţ, T. L. Dragomir, "Solar Cell Parameter Identification Using Genetic Algorithms", Journal of Control Engineering and Applied Informatics, Vol. 12, No. 1, 2010, pp. 30-37.

[20] T. L. Dragomir, D. M. Petreus, F. M. Petcut, I. C. Ciocan, "Comparative analysis of identification methods of the photovoltaic panel characteristics", Proceedings of the IEEE International Conference

on Automation Quality and Testing Robotics, Cluj-Napoca, Romania, 28-30 May 2010, pp. 1-6.

[21] G. J. Yu, Y. S. Jung, J. Y. Choi, G. S. Kim, "A novel two-mode MPPT control algorithm based on comparative study of existing algorithms", Solar Energy, Vol. 76, 2004, pp. 455-463.

[22] V. Jately, S. Arora, "Development of a dual-tracking technique for extracting maximum power from PV systems under rapidly changing environmental conditions", Energy, Vol. 133, 2017, pp. 557-571.

[23] K. Kayisli, "Super twisting sliding mode-type 2 fuzzy MPPT control of solar PV system with parameter optimization under variable irradiance conditions", Ain Shams Engineering Journal, Vol. 14, No. 1, 2023, p. 101950.

[24] V. Jately et al. "Voltage and current reference based MPPT under rapidly changing irradiance and load resistance", IEEE Transactions on Energy Conversion, Vol. 36, No. 3, 2021, pp. 2297-2309.

[25] V. Jately, S. Arora, "An efficient hill-climbing technique for peak power tracking of photovoltaic systems", Proceedings of the IEEE 7th Power India International Conference, Bikaner, India, 25-27 November 2016.